MedChemComm

Accepted Manuscript

ROYAL SOCIETY OF CHEMISTRY

www.rsc.org/medchemcomm

Journal Name

RSCPublishing

COMMUNICATION

Discovery of 2-(5,6-dimethoxypyridin-3-yl)-4-(2,4,6-trifluorobenzyl)-2*H*-pyrido[2,3-*e*][1,2,4]thiadiazin-3(4*H*)-one 1,1-dioxide (HTL6641), a dual orexin receptor antagonist with differentiated pharmacodynamic properties.†

Cite this: DOI: 10.1039/xoxxoooooox

Received ooth January 2012,
Accepted ooth January 2012

DOI: 10.1039/xoxxoooooox

www.rsc.org/

John A. Christopher,[*,a] Sarah J. Aves,[a] Jason Brown,[a] James C. Errey,[a] Suki S. Klair,[b] Christopher J. Langmead,[c] Oliver J. Mace,[a] Richard Mould,[a] Jayesh C. Patel,[a] Benjamin G. Tehan,[a] Andrei Zhukov,[a] Fiona H. Marshall,[a] Miles Congreve.[a]

A novel series of potent, selective, and orally efficacious dual antagonists of the orexin receptors has been investigated, resulting in the identification of lead compound 27 (HTL6641). Comprehensive data for 27 are presented, including *in vivo* PK parameters, confirmation of receptor occupancy through *ex vivo* binding and efficacy in a rat sleep model. A key feature of the series is a short dissociation half-life, measured by surface plasmon resonance (SPR) using stabilized receptors, and confirmed by radioligand-binding experiments. Based on a consideration of the requirements for a potential treatment for insomnia, compound 27 was identified as having the best balance of properties from the chemical series.

The orexin neuropeptides orexin-A and orexin-B, derived from a precursor expressed in the hypothalamus, were independently revealed by two research groups in 1998.[1,2] The orexins bind to two G protein-coupled receptors (GPCRs), OX_1 and OX_2, which are highly conserved across mammalian species, as are the neuropeptides themselves.[1,3] The orexin system is a key regulator of behavioural arousal, sleep and wakefulness. Transgenic mice and rats in which the orexin neurons have been genetically ablated exhibit severe sleepiness, as do orexin peptide knockout mice. In each case a phenotype similar to human narcolepsy patients is observed.[4-6] In humans, loss of the orexin neurons with intact receptor expression is linked to narcolepsy, a chronic sleep disorder characterised by excessive sleepiness during the day, fragmented sleep and cataplexy.[7] In canines, it has been established that disruption of the OX_2 receptor gene results in narcolepsy, providing a clear genetic linkage between the orexin system and sleep modulation.[8]

Over the past decade, there has been a significant drive within the pharmaceutical industry to develop orexin receptor antagonists, with both selective and dual profiles, to investigate the potential for treatment of insomnia, other sleep disorders and other diseases of the central nervous system.[9-12] Current therapies for insomnia treatment centre on the use of benzodiazepines and related derivatives which have sedative, hypnotic and anxiolytic actions resulting from an enhancement of the effect of the neurotransmitter GABA at the $GABA_A$ receptor. Due to a variety of side effects including depression, dependence and sexual dysfunction, and the potential for addiction, benzodiazepine therapies for insomnia are available only on prescription. A related treatment paradigm uses newer drugs such as zolpidem which are positive allosteric modulators of $GABA_A$ receptors and share a similar risk-benefit profile.[13] The strategy of insomnia treatment by modulation of $GABA_A$ receptors is most prominently hampered by CNS-related side effects the morning after administration, including drowsiness, cognitive hang-over effects and a lack of coordination.[14,15] Treatment of insomnia by antagonising orexin receptors presents an opportunity to more directly address the disorder than the existing GABA based therapies, as orexin receptor antagonists, which act to prevent wakefulness, should more selectively regulate the sleep/wake cycle and lack the general CNS depressant effects of current treatments. The majority of efforts in recent years have centred on the

identification and progression of dual orexin receptor antagonists (DORAs), in line with observations that both receptors play a role in regulation of sleep and wakefulness.[16,17] The precise role of the OX_1 receptor remains controversial, as it has been suggested by one group that antagonising the OX_2 receptor alone should have greater efficacy in the treatment of insomnia than a DORA,[18] however both receptors have been found to play different roles in sleep promotion.[19,20] Selective antagonists of either receptor were reviewed in 2013,[21] and more recently OX_2 selective molecules with efficacy in preclinical sleep or antidepressant models have been published by Merck and Eli Lilly respectively.[22,23]

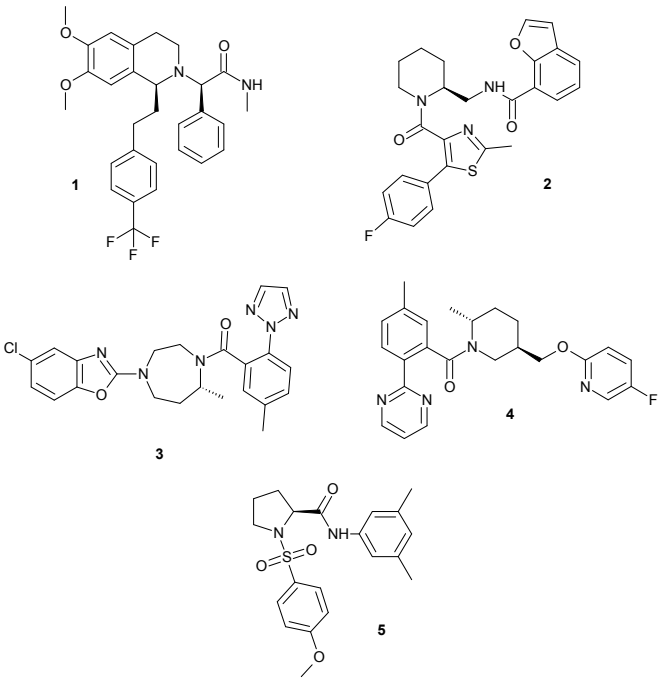

Fig. 1. Clinically evaluated DORAs **1**-**5**.

Several clinical studies have confirmed the therapeutic utility and safety of DORAs in the treatment of insomnia. Almorexant **1** (Fig. 1), developed by Actelion and subsequently licensed to GlaxoSmithKline, demonstrated efficacy in a phase II trial, increasing sleep efficiency in primary insomnia patients.[24] Secondary end points, dose-dependent decreases in latency to persistent sleep (LPS) and wake after sleep onset (WASO), were also met. Although in 2009 almorexant was reported to have achieved its primary end point in an initial phase III trial, development of the molecule was discontinued in 2011 after a review of additional studies conducted to further establish the clinical profile, including tolerability.[25] A second DORA from GSK, SB-649868 **2**, promoted sleep in male insomnia patients, but clinical development was subsequently stopped due to a preclinical safety observation in rats.[26,27] Merck's suvorexant **3** is the most advanced DORA,[28] which was approved for use in adults with insomnia in August 2014. Additionally, Merck have progressed MK-6096 **4** (filorexant) into phase II trials in patients with primary insomnia,[29] and data from Phase I trials of a further DORA from Actelion, ACT-462206 **5**, together with preclinical data, have recently been published.[30,31] The clinical DORAs largely originate from high-throughput screening and it has been challenging to optimize properties such as lipophilicity, for example almorexant has cLogP 5.9,[32] which may be linked to the failure of several compounds due to safety issues unrelated to the mechanism of action.

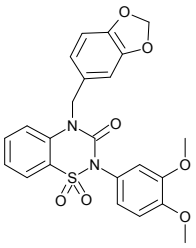

Fig. 2. Initial OX_2 hit **6**.

To develop novel antagonists of the orexin receptors we embarked upon a hit identification campaign using a combination of fragment, focused and virtual screening, selecting several relatively small sets of molecules to screen by surface plasmon resonance (SPR) and/or radioligand binding. A number of promising hits were identified from each approach and several were followed up by further purchasing or synthesis of close analogs. One particular screen of approximately 100 compounds contained molecules selected by medicinal chemists after consideration of how a number of known orexin antagonists were proposed to bind into a refined homology model (see ESI†) of the OX_2 receptor and then targeting molecules considered to have similarity in their pharmacophoric features. The effort uncovered several related hits exemplified by **6** (Fig. 2) which had encouraging binding affinity (OX_2 pK_i 6.6). Compound **6** and several other classes of molecules were selected to test the hypothesis that a central heterocyclic ring containing H-bond acceptors, flanked by two further aromatic substituents which might fold together into a hydrophobically collapsed conformation, would have the potential to bind to the orexin receptors.[33] A number of further commercially available analogs of **6** were available to rapidly build SAR, and synthetic routes were readily amenable to further analog synthesis. An additional attraction of **6** was that the hit was largely dissimilar to known DORAs.[9-12] Initially, a number of analogs which varied the benzyl substituent of **6**, but kept the 3,4-dimethoxyphenyl portion constant, were purchased or synthesized according to the general route in Figure 3. Starting from 2-nitrobenzenesulfonyl chloride, sulfonamide coupling, nitro reduction and cyclisation with triphosgene or 1,1′-carbonyldiimidazole (CDI), yielded benzothiadiazin-3(4*H*)-one 1,1-dioxide intermediates which could then be readily *N*-substituted with benzyl halides or benzyl alcohols. As primary assays for establishing SAR, we used OX_1 and OX_2 radioligand binding assays (see ESI†), focusing our attention primarily on activity at the latter receptor. Data for key early compounds in the series are summarized in Table 1.

Table 1. OX_1 and OX_2 SAR of **7**-**17** (R^1-R^5 = H unless specified). [a] Data represent geometric means of two or more measurements.

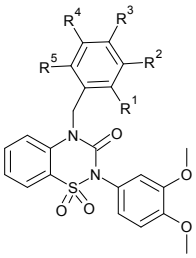

	R^1-R^5	OX_1 pK_i [a]	OX_2 pK_i [a]
7	-	5.7	7.1
8	R^1 = F	6.5	8.2

9	R^1 = F, R^3 = Cl	7.2	8.0
10	R^1 = Cl, R^3 = F	< 5.6	7.6
11	R^1 = Cl, R^5 = F	8.1	9.1
12	R^1, R^3, R^5 = F	7.3	8.7
13	R^1 = Cl, R^3, R^5 = F	7.6	9.0
14	R^1 = OMe, R^3, R^5 = F	7.2	8.2
15	R^1 = Cl, R^3 = Me, R^5 = F	8.2	9.1
16	R^1 = F, R^3 = OMe, R^5 = F	8.7	9.3
17	R^1 = Cl, R^3 = OMe, R^5 = F	9.4	10.0

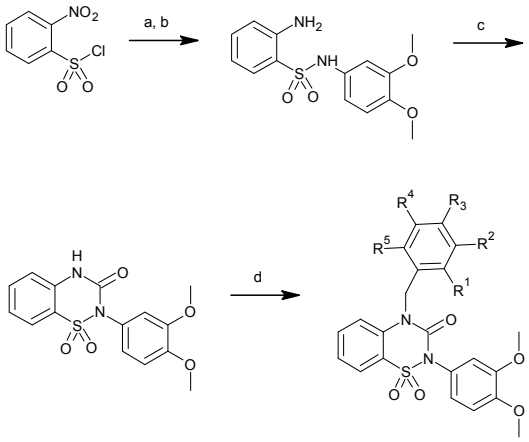

Fig. 3. General synthetic route for synthesis of analogs of **6**. Reagents and conditions: (a) 3,4-dimethoxyaniline, 1,4-dioxane, 80 ºC; (b) $SnCl_2$, EtOH, 100 ºC or Pd/C, H_2, EtOH / H_2O, rt or Fe, AcOH, 60 ºC; (c) triphosgene, 1,4-dioxane, 100 ºC or CDI, Et_3N, DMF, 100 ºC; (d) substituted benzyl alcohol, Ph_3P, diisopropyl azodicarboxylate (DIAD) or 1,1'-azobis(*N*,*N*-dimethylformamide) (TMAD), THF, rt or substituted benzyl halide, K_2CO_3, DMF, 80 ºC.

Removal of the methylenedioxyphenyl unit from **6**, which was deemed undesirable due to a potential bioactivation risk,[34] yielded an improvement in OX_2 affinity for the unsubstituted benzyl analog **7**. Fluorine substitution at the 2-position was favourable (**8**), whereas 3- and 4-fluorination did not increase binding affinity significantly (data not shown). Substitution with chloro at the 2-position was also beneficial. 4-Substitution was envisaged to be advantageous for metabolic stability, and this was tolerated in combination with a 2-substituent (**9**, **10**). 2,6-Disubstitution (**11**) yielded a significant increase in affinity, which was largely maintained in the 2,4,6-trisubstituted analogs **12** and **13**, though not in 2-methoxy derivative **14**. Useful SAR emerged at the 4-position, methyl substitution (**15**) was tolerated in similar fashion to fluoro but installation of methoxy yielded further significant increases in OX_2 affinity (**16** *vs* **12**; **17** *vs* **13**). A range of alkyl and cycloalkyl substitutions in place of the benzyl group were explored, as was replacement of the benzyl by substituted (pyridinyl)methyl groups, but neither strategy yielded sufficient affinity to be explored further (data not shown). In general, analogs exhibited a moderate preference for higher affinity at the OX_2 receptor than OX_1.

Having gained confidence that high affinity could be achieved through optimization of the benzyl group, our attention turned to modification of the 3,4-dimethoxyphenyl unit and the central heterocyclic scaffold, with the primary aim of reducing lipophilicity and obtaining better developability properties within the series. An additional benefit in moving away from the dimethoxyphenyl unit was that the potential for reactive metabolite risks associated with this moiety,[22] or indeed with the presence of a masked aniline, would be removed.

Synthesis in an analogous fashion to the route depicted in Figure 3 allowed replacement of the dimethoxyphenyl group by a variety of dimethoxypyridines. In general this was tolerated (Table 2), with pyridine variants having broadly comparable affinity (compare **18** and **19** to **12**; **20** to **13**). As with the phenyl variants (data not shown), two methoxy substituents were required for high affinity, for example **21** is more than 30-fold less active at OX_2 than the analogous **12**, though as in the phenyl series (data not shown) both 3,4- and 3,5-dimethoxy substitution patterns were well tolerated (**18**, **23** and **19**, **22** respectively). Installation of the pyridine nitrogen at the 2-position was also well tolerated (**24**). Benzyl position SAR was in general highly transferable, and by selection of the most active substituents, OX_2 binding could be readily tuned to high levels, for example **22**, **23** and **24** have affinities in excess of pK_i 9 (K_i < 1 nM).

Table 2

In an exploration of close analogs of the highest affinity compounds, we observed that one or both methoxy groups could be replaced, for example by methyl (data not shown) or methylamino (**25**). In general, when compared directly to the methoxy analogs (data not shown), up to a 10-fold loss of OX_2 affinity was observed, and the majority of these changes also resulted in a significant loss of *in vitro* metabolic stability. Changes to the thiadiazin-3(4*H*)-one 1,1-dioxide portion of the central scaffold were poorly tolerated, for example **28**, Table 2, whereas modification of the fused phenyl portion was more encouraging. Most notably, installation of a nitrogen atom at the 5-position allowed the lipophilicity of the series to be decreased whilst maintaining high levels of OX_1 and OX_2 binding affinity (**25-27**, Table 2). 5-Aza analogs of this type could be readily accessed from 2-chloropyridine-3-sulfonyl chloride using the synthetic route depicted in Figure 4, with sulfonamide coupling preceding S_NAr reaction with a substituted benzylamine, followed by ring closure with triphosgene or CDI.

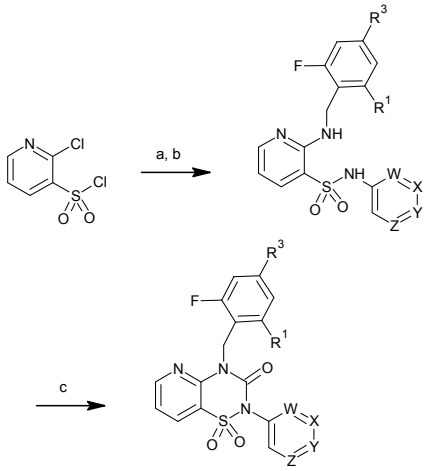

Fig. 4. Synthesis of **25-27**. Reagents and conditions: (a) Heteroaryl amine, pyridine, DCM, 0 ºC or Heteroaryl amine, 1,4-dioxane, 0 ºC; (b) Substituted benzylamine, MeCN, microwave heating, 180 ºC, 1-2 h; (c) triphosgene, 1,4-dioxane, 100 ºC or CDI, Et_3N, DMF, 100 ºC.

An important consideration that we were aware of during the course of the project is that the duration of action *in vivo* of orexin antagonists will be dependent upon both the pharmacokinetic and receptor-ligand kinetic parameters of the molecule. Pharmacokinetic parameters are an important consideration during medicinal chemistry optimization, however whilst these measurements are routine it is not always the case that pharmacodynamic effects are

measured at the level of the receptor.[35,36] At Heptares we use biochemical and/or biophysical approaches to routinely probe structure-kinetic relationships (SKR) to enable us to select molecules with appropriate attributes for progression. A notable feature of the advanced DORAs suvorexant and almorexant is that they exhibit slow kinetics at the orexin receptors.[37,38] In the treatment of sleep disorders, a potential issue for compounds with slow receptor kinetics is that they may exhibit a prolonged duration of action which could potentially promote next-day residual effects. Therefore, as part of our progression strategy we sought to identify molecules with appropriate parameters, both in terms of moderate pharmacokinetic half-lives and a fast receptor off-rate.

To address these twin challenges, we first examined examples of our series in biophysical and biochemical assays to determine receptor binding kinetics. Wild-type GPCRs are rarely stable enough to be successfully captured on to biosensor chips for evaluation by SPR,[39] a limitation which can be successfully overcome by increasing thermostability through protein engineering.[40,41] Introduction of a small number of mutations, which do not affect the binding site characteristics of the receptor but dramatically increase thermostability, yield modified GPCRs known as StaR® proteins. The stabilized receptors can be successfully immobilized on biosensor chips and used for fragment screening,[42] Biophysical Mapping™,[43] and for evaluation of receptor-ligand kinetic parameters,[44] as we have previously described. OX_1 and OX_2 StaR proteins were generated which had significantly increased thermostability and retained the ligand binding characteristics of the wild-type receptors.[40] The enhanced stability of the purified proteins allowed capture on SPR sensor chips (see ESI†) and examination of the kinetics of receptor-ligand binding interactions of standard molecules and multiple compounds in our series. Dilution series of each compound were injected, and blank-subtracted data were fitted to a 1:1 interaction model to obtain kinetic and affinity constants. Our series, exemplified by **18** and **27**, displayed fast OX_2 receptor kinetics, with **18** (see ESI†) having an on rate (k_a) of $2.8x10^4$ $M^{-1}s^{-1}$, an off rate (k_d) of $2.7x10^{-3}$ s^{-1} and a dissociation half-life ($t_{1/2}$ = (ln $2/k_d$)/60) of 4.3 min. The close analog **27** (Figure 5) was profiled at both the OX_1 (k_a $2.0x10^4$ $M^{-1}s^{-1}$, k_d $1.6x10^{-2}$ s^{-1}, $t_{1/2}$ = 0.8 min) and OX_2 receptors (k_a $3.3x10^4$ $M^{-1}s^{-1}$, k_d $2.8x10^{-3}$ s^{-1}, $t_{1/2}$ = 4.2 min). Suvorexant by comparison displayed much slower receptor kinetics with dissociation half-lives of 24 and 210 min for the OX_1 and OX_2 receptors respectively. Evaluation of OX_2 receptor kinetics using Motulsky-Mahan radioligand-binding studies was also undertaken,[38,45] and yielded comparable data: **18** $t_{1/2}$ = 3.0 min; **27** $t_{1/2}$ = 7.6 min; suvorexant $t_{1/2}$ = 79 min; the latter figure is additionally in line with that reported in the literature by workers from Merck.[37] In OX_2 radioligand-binding studies almorexant has a dissociation half-life of 242 min.[38] The significantly faster receptor kinetics observed with members of our series including **18** and **27** should facilitate rapid re-equilibration with changing orexin levels *in vivo*, to help reduce the potential risk for next day somnolence effects.[37]

During the medicinal chemistry progression of the series described herein, in addition to the studies presented in this manuscript, multiple co-crystal structures of compounds from the benzothiadiazine series, another novel series from our laboratories, and literature compounds such as suvorexant and SB-334867,[46] were solved in complex with OX_1 and/or OX_2 StaR proteins. These crystal structures revealed, in fine detail, the binding modes of the various series and how they relate to one another, as well as giving some insight into the binding kinetics of the receptors. In particular the X-ray structures provided a detailed understanding of the differences between the two receptors and have been used extensively to inform further iterations of our medicinal chemistry project leading to the design of uniquely selective OX_1 antagonists which have potential in the treatment of addiction disorders.[47] These data are beyond the scope of this communication and will be the subject of future publications in specialized journals. During the preparation of this manuscript, the crystal structure of suvorexant bound to an OX_2 fusion protein construct was disclosed.[48]

Figure 5. (a) OX_1 and (b) OX_2 Surface Plasmon Resonance sensorgrams of **27**.

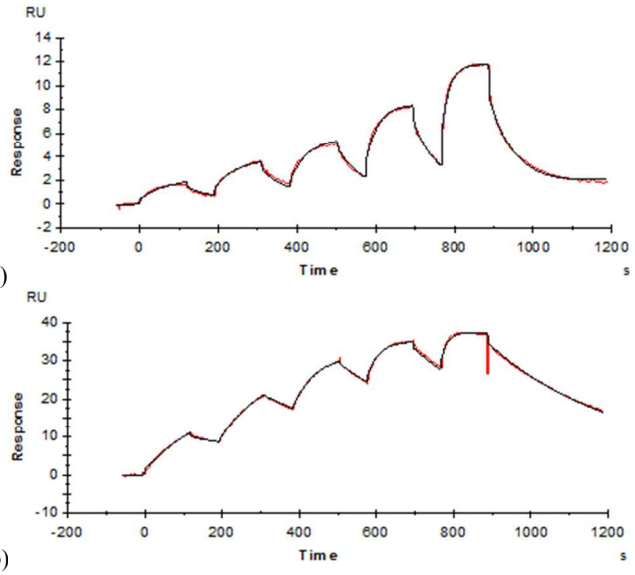

In parallel with profiling key compounds through standard *in vitro* assays such as the hERG ion channel and P450 inhibition we routinely monitored *in vitro* stability in rat-liver microsomal preparations (RLM $t_{1/2}$, Table 2). For the reasons detailed above, we needed to strike a delicate balance between having sufficient metabolic stability to not compromise oral bioavailability through high first-pass metabolism, yet having a relatively short pharmacokinetic half-life in rat as an initial pre-clinical species. Profiling of early molecules in PK experiments in male Sprague Dawley rats by both iv and po routes allowed us to identify a half-life range in the RLM assay of 15-35 minutes as an appropriate criteria for progression; data for key advanced compounds are summarized in Table 3. Compound **18** and the regioisomeric **19** have low *in vivo* clearance (18 and 17 mL/min/kg respectively) with **18** having a shorter half-life by virtue of a lower volume of distribution than **19**. In line with its higher measured plasma protein binding (PPB) in rat, an additional *in vitro* parameter which we closely monitored during series progression, **19** additionally compares poorly to its regioisomer in terms of the unbound fraction in the brain (approximated as the ratio of drug concentration in the cerebrospinal fluid (CSF) to that in brain at the same time point);[49] in common with the majority of compounds profiled, both molecules had very good brain penetration. Chloro derivative **20**, with both higher clearance and volume of distribution than **18**, had a similar half-life and a higher free fraction in brain. All three molecules, together with the aza-examples **26** and **27**, had acceptable oral bioavailability (29-66%). Selected compounds were additionally progressed to PK studies in male beagles; **18** had low clearance, moderate volume of distribution, long half-life and excellent bioavailability. Compound **27**, the aza-variant of **18**, also had a good profile in beagle with moderate clearance and volume of distribution,

good bioavailability and a shorter half-life than **18**. The mean residence time (MRT) of **27** was 1.9 h and 4.0 h in rat and beagle, respectively. Overall, these PK parameters suggest a short to moderate half-life in human.

Table 3

After consideration of the overall profiles of **27** and related close analogs, **27** was selected for extensive further profiling as summarized below and in Table 4. The dual-antagonist profile of **27** was confirmed in OX_1 and OX_2 antagonist functional cell assays measuring receptor-stimulated ERK1/2 phosphorylation. A clean *in vitro* profile was apparent, with no issues identified with inhibition of P450 isoforms or the hERG ion channel. Evaluation of bidirectional apparent permeability (P_{app}) across a Caco-2 cell monolayer indicated that the molecule had high passive permeability with low efflux. Binding to human, dog and mouse plasma proteins was high, in common with the measured value in rat (99.5%), and the latter is consistent with the CSF concentrations observed in rat PK experiments. Evaluation of suvorexant as a benchmark in these assays returned comparable data (99.4, 98.3, 99.3% for human, dog and mouse respectively). Screening in an *in vitro* cytotoxicity assay in HepG2 cells, determining cell viability by ATP measurements, revealed no issues, and the molecule was inactive in a 5-strain AMES test with and without S9 fractions. Stability in human, cynomolgus monkey, dog and rat hepatocytes was high, and subsequently the major metabolites arising from incubation with hepatocytes from these four species were characterized. In all species mono-demethylation of **27** was the major metabolite, with subsequent glucuronide conjugation also observed. Low levels of mono-oxidation, with and without sulfation or glucuronidation, were also noted. The two regioisomeric de-methylated metabolites of **27** were synthesized and profiled in binding assays, and in each case a significant drop in affinity (approximately 80-fold) compared to the parent was observed, suggesting a low risk of active metabolite formation *in vivo*. No metabolites that were unique to human were observed, and there was no evidence of addition of glutathione to the parent molecule or metabolites, which would be indicative of a risk of formation of a reactive metabolite. Cross-screening of **27** in a small number of in-house GPCR radioligand binding assays (M_1, M_2, M_3, M_4, CGRP, GLP1, $mGlu_5$) provided initial confidence that the molecule had good selectivity for the OX receptors. Wider profiling in an external panel of 14 GPCR, kinase, ion-channel and nuclear receptor targets indicated that **27** had at least 1,000 fold selectivity against the panel members. Compound **18**, a close analog of **27**, had been earlier screened against an extended panel of 68 targets and also had excellent selectivity, providing overall confidence in the selectivity of the chemotype.

Table 4

With these data in hand, **27** was advanced to a rat *ex vivo* autoradiography experiment (RenaSci Ltd, Nottingham, UK) to evaluate OX_2 receptor occupancy in the CNS from an oral dose. Male Sprague Dawley rats were dosed orally with vehicle alone (10% DMA, 10% Solutol HS15, 80% (10% aqueous (2-hydroxypropyl)-β-cyclodextrin)) or **27** (1 mg/kg, po) and sacrificed 1 h post-dose. Frontal cortex sections were prepared and incubated with [^{3}H]EMPA,[50] with levels of bound radioactivity in the sections determined using a beta imager. Receptor occupancy was determined from mean specific binding with the vehicle treated control taken as 100%. In this study **27** demonstrated a mean receptor occupancy of 57% from an oral dose of 1 mg/kg (Figure 6); by comparison, suvorexant from a 1 mg/kg oral dose achieved 31% receptor occupancy. Plasma exposures at this time point were 72 ng/mL and 22 ng/mL for **27** and suvorexant respectively. The study confirmed that despite the fast receptor kinetics of **27**, high occupancy of the OX_2 receptors could be achieved from an oral dose.

The effect of **27** treatment on rat sleep architecture *in vivo* was investigated using a telemetered CT18 sleep study (Aptuit (Verona) Srl., Italy), a model which has previously been used to support orexin lead optimisation programmes prior to positive clinical proof of concept in insomnia patients.[51] Adult male CD rats were implanted with telemetric probes to record electroencephalogram (EEG) and neck electromyogram (EMG) readings. The study employed a balanced cross-over design in which all animals were alternatively treated with drug and vehicle. Rats were dosed with vehicle (80% PEG-400 and 20% Cremophor® EL) or with **27** (3 and 10 mg/kg) po, administered at circadian time 18h (CT18, six hours after lights off). The effect of **27** on sleep patterns was evaluated starting the recording 6 hours in to the dark phase. EEG and neck EMG readings were recorded and analysed for 5 hours after treatment to determine time spent awake, NREM and REM sleep (Figure 7A – C). Sleep and wake stages in rats were altered by **27** compared to vehicle, with the hypnotic effect of **27** starting to decline after 3 hours. Peak effects on sleep parameters occurred at approximately 2 h, in contrast to a T_{max} of approximately 0.5 h in the rat oral PK study, and a clear dose response in several of the sleep parameters examined was not apparent. Given the limitations of this initial study further *in* vivo efficacy experiments are warranted to better understand the properties of **27**. During episodes of insomnia, it is important to decrease the time spent awake during the night, a clinical end point measured during a sleep trial, as well as increasing the duration of sleep. At 3 and 10 mg/kg, **27** promoted sleep and reduced the time spent awake by 17.4 and 18.5% ($p < 0.05$; Figure 7D), respectively, over 3 hours. The time spent asleep was also significantly increased by both doses of **27**, which promoted sleep primarily by increasing REM, with smaller effects on NREM. Over 3 hours, the time spent in REM sleep over 3 hours was significantly increased by 70.6 and 69.6% ($p < 0.01$; Figure 7F) by 3 and 10 mg/kg **27**. The time spent in NREM sleep was increased by 28.8 and 30.7% ($p < 0.05$; Figure 7E) at 3 and 10 mg/kg **27**, respectively. Consistent with a smaller effect on NREM, there was no significant effect on the latency to the first NREM episode following treatment with **27** at the doses tested (Figure 7G). However, the latency to the first REM episode was reduced by treatment with 10 mg/kg **27**, reducing the time taken by 35.0% from 70.9 ± 7.7 to 46.1 ± 6.6 mins ($p < 0.05$; Figure 7H) compared to vehicle. In a similar rat sleep model, suvorexant demonstrated significant changes in sleep architecture from a 30 mg/kg dose with greater effects on REM than NREM, providing overall confidence that **27** demonstrates encouraging efficacy *in vivo*.[52]

Figure 6. [^{3}H]EMPA *ex vivo* autoradiography in rat frontal cortex 1 hour following oral administration of **27** and suvorexant at 1 mg/kg.

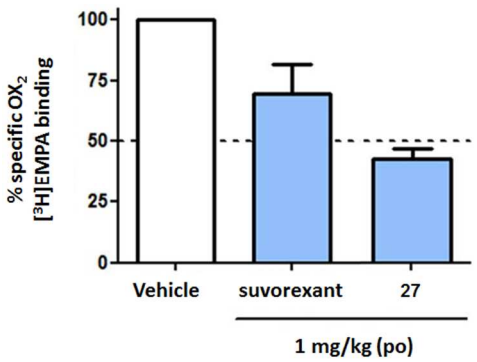

Figure 7. Telemetered rat circadian time (CT) 18 sleep study of **27**.

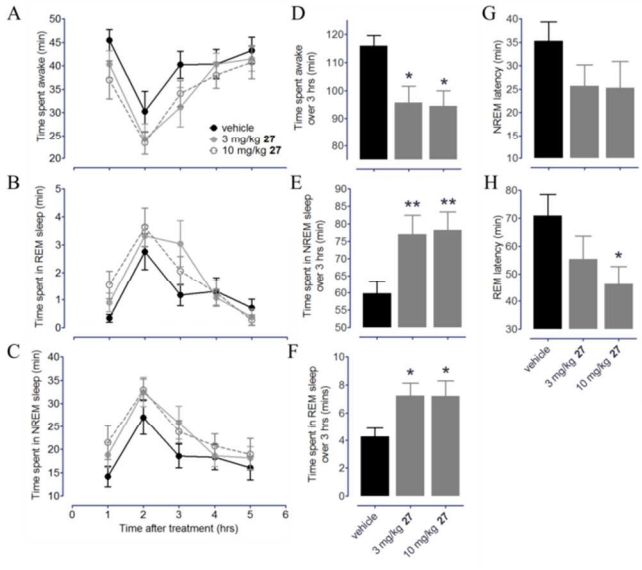

Conclusions

In summary, the series described herein, exemplified by compounds such as **18** and **27**, represents a novel, high affinity dual orexin receptor antagonist chemotype, with a good overall *in vitro* and *in vivo* developability profile. Based on a consideration of the requirements for a potential treatment for insomnia, compound **27** (HTL6641), was identified as having the best balance of properties in the chemical series. Key factors which warrant the further investigation of **27** are its appropriate pre-clinical PK profile, high CNS receptor occupancy, fast off-rate kinetics and relevant *in vivo* efficacy in a rat sleep study.

Experimental details

All studies involving live animals were performed in compliance with national laws and institutional guidelines, following approval by the relevant committees of the study centres.

Synthetic methods. The purity of the final compounds was determined by LC/MS analysis to be ≥95%. Supplier information for purchased compounds, LCMS QC data for all compounds, experimental details and ^{1}H NMR data for all synthesized compounds in Tables 1 and 2 are described in the ESI †. Suvorexant was synthesized in accordance with literature conditions.[53] *J* values are given in Hz. Synthesis of **27** is described below.

2-Chloro-N-(5,6-dimethoxypyridin-3-yl)pyridine-3-sulfonamide. A mixture of 2-chloropyridine-3-sulfonyl chloride (530 mg, 2.50 mmol), 5,6-dimethoxypyridin-3-amine (424 mg, 2.75 mmol) and pyridine (0.60 mL, 7.42 mmol) in DCM (10 mL) was stirred at 0ºC for 3 h before concentration *in vacuo*. Purification by gradient column chromatography, eluting with 12-60% EtOAc in iso-hexane yielded the title compound (542 mg, 1.64 mmol, 66%) as a pale orange solid. m/z 328.2, 330.2 $(M-H)^-$; δ_H (400 MHz; d_6-DMSO) 3.70 (3 H, s), 3.77 (3 H, s), 7.02 (1 H, d, *J* 2.3), 7.39 (1 H, d, *J* 2.3), 7.61 (1 H, dd, *J* 7.9, 4.8), 8.38 (1 H, dd, *J* 7.9, 1.8), 8.64 (1 H, dd, *J* 4.8, 1.8), 10.71 (1 H, s).

N-(5,6-Dimethoxypyridin-3-yl)-2-[(2,4,6-trifluorobenzyl)amino]pyridine-3-sulfonamide. A mixture of 2-chloro-*N*-(5,6-dimethoxypyridin-3-yl)pyridine-3-sulfonamide (165 mg, 0.50 mmol) and 2,4,6-trifluorobenzylamine (0.18 mL, 1.47 mmol) in MeCN (3 mL) was heated in a microwave reactor at 180 ºC for 1 h. After concentration *in vacuo* purification by gradient column chromatography, eluting with 7-60% EtOAc in iso-hexane yielded the title compound (218 mg, 0.48 mmol, 96%) as a yellow oil. m/z 453.2 $(M-H)^-$; δ_H (400 MHz; d_6-DMSO) 3.62 (3 H, s), 3.73 (3 H, s), 4.60 (2 H, d, *J* 5.5), 6.49-6.72 (2 H, m), 6.83 (1 H, d, *J* 2.3), 7.14 (2 H, t, *J* 8.7), 7.21 (1 H, d, *J* 2.3), 7.78 (1 H, dd, *J* 7.8, 1.8), 8.22 (1 H, dd, *J* 4.8, 1.6), 10.27 (1 H, s).

*2-(5,6-Dimethoxypyridin-3-yl)-4-(2,4,6-trifluorobenzyl)-2H-pyrido[2,3-e][1,2,4]thiadiazin-3(4H)-one 1,1-dioxide (**27**, HTL6641)*. A mixture of *N*-(5,6-dimethoxypyridin-3-yl)-2-[(2,4,6-trifluorobenzyl)amino]pyridine-3-sulfonamide (218 mg, 0.48 mmol), 1,1′-carbonyldiimidazole (311 mg, 1.92 mmol) and triethylamine (0.13 mL, 0.93 mmol) in DMF (1.5 mL) in a sealed tube was heated at 100 ºC for 2 h. After concentration in vacuo purification by gradient column chromatography, eluting with 10-80% EtOAc in iso-hexane yielded the title compound (159 mg, 0.33 mmol, 69%) as a white solid. m/z 481.1 $(M+H)^+$; δ_H (400 MHz; d_6-DMSO) 3.77 (3 H, s), 3.93 (3 H, s), 5.59 (2 H, s), 7.19 (2 H, t, *J* 8.8), 7.35 (1 H, d, *J* 2.0), 7.53 (1 H, dd, *J* 7.8, 4.8), 7.75 (1 H, d, *J* 2.0), 8.51 (1 H, dd, *J* 7.8, 1.8), 8.85 (1 H, dd, *J* 4.9, 1.6); δ_F (376 MHz; d_6-DMSO, $C_6H_5CF_3$) -111.0 (1 F), -113.6 (2 F); δ_C (101 MHz; CD_3CN) 36.8 (1 C), 54.5 (1 C), 56.7 (1 C), 101.3 (2 C, ddd, $^2J_{CF}$ 26.1, $^2J_{CF}$ 26.1, $^4J_{CF}$ 2.3), 110.4 (1 C, td, $^2J_{CF}$ 18.4, $^4J_{CF}$ 4.6), 119.9, 120.8, 122.1, 122.9, 133.7 (1 C), 138.8 (1 C), 145.6 (1 C), 147.9 (1 C), 151.0 (1 C), 154.4 (1 C), 156.3 (1 C), 162.9 (2 C, ddd, $^1J_{CF}$ 249.6, $^3J_{CF}$ 15.3, $^3J_{CF}$ 11.1), 163.3 (1 C, dt, $^1J_{CF}$ 247.7, $^3J_{CF}$ 16.1).

ACKNOWLEDGEMENTS

Giles A. Brown is acknowledged for assistance with radioligand and suvorexant synthesis. Members of the Heptares pharmacology group are acknowledged for the generation of selectivity data for HTL6641. Liz Jagger and colleagues at RenaSci Ltd are acknowledged for generation of *ex vivo* autoradiography data, and Laura Piccoli and colleagues at Aptuit (Verona) Srl. are acknowledged for generation of data from the CT18 sleep study.

Notes and references

[a] Heptares Therapeutics Ltd., BioPark, Welwyn Garden City, Hertfordshire, AL7 3AX, U.K.‡

[b] Labstract Ltd., Stevenage Bioscience Catalyst, Gunnels Wood Road, Stevenage, Hertfordshire, SG1 2FX, U.K.

[c] Monash Institute of Pharmaceutical Sciences, Monash University, 381 Royal Parade, Parkville 3052, Victoria, Australia.

† Electronic Supplementary Information (ESI) available. See DOI: 10.1039/c000000x/

1 T. Sakurai, A. Amemiya, M. Ishii, I. Matsuzaki, R. M. Chemelli, H. Tanaka, S. C. Williams, J. A. Richardson, G. P. Kozlowski, S. Wilson, J. R. S. Arch, R. E. Buckingham, A. C. Haynes, S. A. Carr, R. S. Annan, D. E. McNulty, W.-S. Liu, J. A. Terrett, N. A. Elshourbagy, D. J. Bergsma, and M. Yanagisawa, *Cell*, 1998, **92**, 573.

2 L. de Lecea, T. S. Kilduff, C. Peyron, X.-B. Gao, P. E. Foye, P. E. Danielson, C. Fukuhara, E. L. F. Battenberg, V. T. Gautvik, F. S. Bartlett II, W. N. Frankel, A. N. van Den Pol, F. E. Bloom, K. M. Gautvik and J. G. Sutcliffe, *Proc. Natl. Acad. Sci. U.S.A.*, 1998, **95**, 322.

3 J. Gatfield, C. Brisbare-Roch, F. Jenck and C. Boss, *ChemMedChem*, 2010, **5**, 1197.

4 R. M. Chemelli, J. T. Willie, C. M. Sinton, J. K. Elmquist, T. Scammell, C. Lee, J. A. Richardson, S. C. Williams, Y. Xiong, Y. Kisanuki, T. E. Fitch, M. Nakazato, R. E. Hammer, C. B. Saper, and M. Yanagisawa, *Cell*, 1999, **98**, 437.

5 C. T. Beuckmann, C. M. Sinton, S. C. Williams, J. A. Richardson, R. E. Hammer, T. Sakurai and M. Yanagisawa, *J. Neurosci*., 2004, **24**, 4469.

6 J. Hara, C. T. Beuckmann, T. Nambu, J. T. Willie, R. M. Chemelli, C. M. Sinton, F. Sugiyama, K.-i. Yagami, K. Goto, M. Yanagisawa and T. Sakurai, *Neuron*, 2001, **30**, 345.

7 N. Tsujino and T. Sakurai, *Pharmacol. Rev*., 2009, **61**, 162.

8 L. Lin, J. Faraco, R. Li, H. Kadotani, W. Rogers, X. Lin, X. Qiu, P. J. de Jong, S. Nishino and E. Mignot, *Cell*, 1999, **98**, 365.

9 P. J. Coleman, and J. J. Renger, *Expert Opin. Ther. Patents*, 2010, **20**, 307.

10 J. A. Christopher, *Pharm. Pat. Analyst*., 2012, **1**, 329.

11 C. Boss, *Expert Opin. Ther. Patents*, 2014, **24**, 1367

12 J. A. Christopher, *Pharm. Pat. Analyst*., 2014, **3**, 625.

13 J. Wagner, M. L. Wagner, and W. A. Hening, *Ann. Pharmacother*., 1998, **32**, 680.

14 R. Hoque and A. L. Chesson, *J. Clin. Sleep Med*., 2009, **5**, 471.

15 T. Roehrs and T. Roth, *Neurotherapeutics*, 2012, **9**, 728.

16 J. T. Willie, R. M. Chemelli, C. M. Sinton, S. Tokita, S. C. Williams, Y. Y. Kisanuki, J. N. Marcus, C. Lee, J. K. Elmquist, K. A. Kohlmeier, C. S. Leonard, J. A. Richardson, R. E. Hammer and M. Yanagisawa, *Neuron*, 2003, **38**, 715.

17 S. R. Morairty, F. G. Revel, P. Malherbe, J.-L. Moreau, D. Valladao, D, J. G. Wettstein, T. S. Kilduff and E. Borroni, *PLoS ONE*, [Online] 2012, **7**, e39131.

18 C. Dugovic, J. E. Shelton, L. E. Aluisio, I. C. Fraser, X. Jiang, S. W. Sutton, P. Bonaventure, S. Yun, X. Li, B. Lord, C. A. Dvorak, N. I. Carruthers and T. W. Lovenberg, *J. Pharmacol. Exp. Ther.*, 2009, **330**, 141.

19 C. Dugovic, J. E. Shelton, S. Yun, P. Bonaventure, B. T. Shireman and T. W. Lovenberg, *Front. Neurosci.*, [Online] 2014, **8**, Article 28.

20 K. Etori, Y. C. Saito, N. Tsujino and T. Sakurai, *Front. Neurosci.*, [Online] 2014, **8**, Article 8.

21 T. P. Lebold, P. Bonaventure and B. T. Shireman, *Bioorg. Med. Chem. Lett*., 2013, **23**, 4761.

22 A. J. Roecker, S. P. Mercer, J. D. Schreier, C. D. Cox, M. E. Fraley, J. T. Steen, W. Lemaire, J. G. Bruno, C. M. Harrell, S. L. Garson, A. L. Gotter, S. V. Fox, J. Stevens, P. L. Tannenbaum, T. Prueksaritanont, T. D. Cabalu, D. Cui, J. Stellabott, G. D. Hartman, S. D. Young, C. J. Winrow, J. J. Renger and P. J. Coleman, *ChemMedChem*, 2014, **9**, 311.

23 T. E. Fitch, M. J. Benvenga, C. D. Jesudason, C. Zink, A. B. Vandergriff, M. M. Menezes, D. A. Schober and L. M. Rorick-Kehn, *Front. Neurosci.*, [Online] 2014, **8**, Article 5.

24 P. Hoever, G. Dorffner, H. Beneš, T. Penzel, H. Danker-Hopfe, M. J. Barbanoj, G. Pillar, B. Saletu, O. Polo, D. Kunz, J. Zeitlhofer, S. Berg, M. Partinen, C. L. Bassetti, B. Högl, I. O. Ebrahim, E. Holsboer-Trachsler, H. Bengtsson, Y. Peker, U.-M. Hemmeter, E. Chiossi, G. Hajak and J. Dingemanse, *Clin. Pharmacol. Ther*., 2012, **91**, 975.

25 GlaxoSmithKline press release. http://www.gsk.com/en-gb/media/press-releases/2011/gsk-and-actelion-discontinue-clinical-development-of-almorexant (accessed January 15, 2015).

26 P. B. Bettica, L. Squassante, S. Zamuner, G. Nucci, H. Danker-Hopfe and E. Ratti, *Sleep*, 2012, **35**, 1097.

27 ClinicalTrials record. http://clinicaltrials.gov/ct2/show/NCT00534872?term=SB-649868&rank=1 (accessed January 15, 2015).

28 W. J. Herring, K. M. Connor, N. Ivgy-May, E. Snyder, K. Liu, D. B. Snavely, A. D. Krystal, J. K. Walsh, R. M. Benca, R. Rosenberg, R. B. Sangal, K. Budd, J. Hutzelmann, H. Leibensperger, S. Froman, C. Lines, T. Roth and David Michelson, *Biol. Psychol*., 2014, DOI:10.1016/j.biopsych.2014.10.003.

29 P. J. Coleman, J. D. Schreier, C. D. Cox, M. J. Breslin, D. B. Whitman, M. J. Bogusky, G. B. McGaughey, R. A. Bednar, W. Lemaire, S. M. Doran, S. V. Fox, S. L. Garson, A. L. Gotter, C. M. Harrell, D. R. Reiss, T. D. Cabalu, D. Cui, T. Prueksaritanont, J. Stevens, P. L. Tannenbaum, R. G. Ball, J. Stellabott, S. D. Young, G. D. Hartman, C. J. Winrow and J. J. Renger, *ChemMedChem*, 2012, **7**, 415.

30 M. Hoch, H. van Gorsel, J. van Gerven and J. Dingemanse, *J. Clin. Pharmacol.*, 2014, **54**, 979

31 C. Boss, C. Roch-Brisbare, M. A. Steiner, A. Treiber, H. Dietrich, F. Jenck, M. von Raumer, T. Sifferlen, C. Brotschi, B. Heidmann, J. T. Williams, H. Aissaoui, R. Siegrist, and J. Gatfield, *ChemMedChem*, 2014, **9**, 2486.

32 ACD/LogP calculator, version 12.02, within ACD/ChemSketch, release 12.00, was used to calculate cLogP values. http://www.acdlabs.com.

33 C. D. Cox, G. B. McGaughey M. J. Bogusky D. B. Whitman, R. G. Ball, C. J. Winrow, J. J. Renger and P. J. Coleman, *Bioorg. Med. Chem. Lett.*, 2009, **19**, 2997.

34 A. S. Kalgutkar, I. Gardner, R. S. Obach, C. L. Shaffer, E. Callegari, K. R. Henne, A. E. Mutlib, D. K. Dalvie, J. S. Lee, Y. Nakai, J. P. O'Donnel, J. Boer and S. P. Harriman, *Curr. Drug Metab*., 2005, **6**, 161.

35 R. Zhang and F. Monsma, *Curr. Opin. Drug Discov. Dev*., 2009, **12**, 488.

36 R. A. Copeland, *Expert Opin. Drug Discov*., 2010, **5**, 305.

37 A. L. Gotter, C. J. Winrow, J. Brunner, S. L. Garson, S. V. Fox, J. Binns, C. M. Harrell, D. Cui, K. L. Yee, M. Stiteler, J. Stevens, A. Savitz,

P. L. Tannenbaum, S. J. Tye, T. McDonald, L. Yao, S. D. Kuduk, J. Uslaner, P. J. Coleman, J. J. Renger, *BMC Neuroscience* [Online], 2013, **14**, 90.

38 R. Mould, J. Brown, F. H. Marshall and C. J. Langmead, *Br. J. Pharmacol.*, 2014, **171**, 351.

39 S. G. Patching, *Biochim. Biophys. Acta*, 2014, **1838**, 43.

40 N. Robertson, A. Jazayeri, J. Errey, A. Baig, E. Hurrell, A. Zhukov, C. J. Langmead, M. Weir and F. H. Marshall, *Neuropharmacology*, 2011, **60**, 36.

41 M. Congreve, R. L. Rich, D. G. Myszka, F. Figaroa, G. Siegal and F. H. Marshall, in *Methods in Enzymology*, ed. L. C. Kuo, Academic Press, Burlington, MA, U.S., 2011, vol. 493, ch. 5, pp 115−136.

42 J. A. Christopher, J. Brown, J.; A. S. Doré, J. C. Errey, M. Koglin, F. H. Marshall, D. G. Myszka, R. L. Rich, C. G. Tate, B. Tehan, T. Warne, and M. Congreve, *J. Med. Chem*., 2013, **56**, 3446.

43 A. Zhukov, S. P. Andrews, J. C. Errey, N. Robertson, B. Tehan, J. S. Mason, F. H. Marshall, M. Weir and M. Congreve, *J. Med. Chem*., 2011, **54**, 4312.

44 M. Congreve, S. P. Andrews, A. S. Doré, K. Hollenstein, E. Hurrell, C. J. Langmead, J. S. Mason, I. W. Ng, B. Tehan, A. Zhukov, M. Weir and F. H. Marshall, *J. Med. Chem*., 2012, **55**, 1898.

45 H. J. Motulsky and L. C. Mahan, *Mol. Pharmacol*., 1984, **25**, 1.

46 R. A. Porter, W. N. Chan, S. Coulton, A. Johns, M. S. Hadley, K. Widdowson, J. C. Jerman, S. J. Brough, M. Coldwell, D. Smart, F. Jewitt, P. Jeffrey and N. Austin, *Bioorg. Med. Chem. Lett*., 2001, **11**, 1907.

47 C. Baimel, S. E. Bartlett, L.-C. Chiou, A. J. Lawrence, J. W. Muschamp, O. Patkar, L.-W. Tung and S. L. Borgland, *Br. J. Pharm.*, 2015, **172**, 334.

48 J. Yin, J. C. Mobarec, P. Kolb and D. M. Rosenbaum, *Nature*, 2015, DOI:10.1038/nature14035.

49 Z. Rankovic, *J. Med. Chem*., 2015, DOI: 10.1021/jm501535r.

50 P. Malherbe, E. Borroni, L. Gobbi, H. Knust, M. Nettekoven, E. Pinard, O. Roche, M. Rogers-Evans, J. G. Wettstein and J.-L. Moreau, *J. Pharmacol.*, 2009, **156**, 1326–1341.

51 P. A. Gerrard, R. Porter, V. Holland, M. Massagrande, A. Poffe, L. Piccoli, P. Bettica, M. Corsi, F. Hagan, J. Hagan and E. Ratti, *Sleep*, 2009, **32** (Suppl. 0125), A42.

52 C. D. Cox, M. J. Breslin, D. B. Whitman, J. D. Schreier, G. B. McGaughey, M. J. Bogusky, A. J. Roecker, S. P. Mercer, R. A. Bednar, W. Lemaire, J. G. Bruno, D. R. Reiss, C. M. Harrell, K. L. Murphy, S. L. Garson, S. M. Doran, T. Prueksaritanont, W. B. Anderson, C. Tang, S. Roller, T. D. Cabalu, D. Cui, G. D. Hartman, S. D. Young, K. S. Koblan, C. J. Winrow, J. J. Renger and P. J. Coleman, *J. Med. Chem.*, 2010, **53**, 5320.

53 C. A. Baxter, E. Cleator, K. M. J. Brands, J. S. Edwards, R. A. Reamer, F. J. Sheen, G. W. Stewart, N. A. Strotman and D. J. Wallace, *Org. Process Res. Dev*., 2011, **15**, 367.

Table 2. OX_1 and OX_2 SAR and rat microsomal stability of **18-28**. [a] Data represent geometric means of two or more measurements, *nd* = not determined. [b] Reference 32.

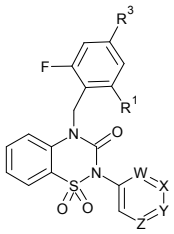

18-24

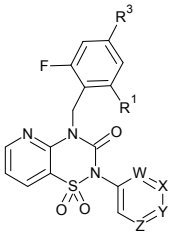

25-27

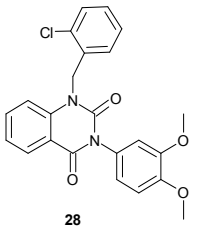

28

	R^1	R^3	W	X	Y	Z	OX_1 pK_i [a]	OX_2 pK_i [a]	RLM $t_{1/2}$ (min)	cLogP [b]
18	F	F	CH	N	COMe	COMe	7.9	8.3	28	2.9
19	F	F	CH	COMe	N	COMe	7.8	8.9	16	3.1
20	Cl	F	CH	N	COMe	COMe	7.4	8.8	23	2.5
21	F	F	CH	COMe	N	CH	6.4	7.2	23	2.7
22	F	OMe	CH	COMe	N	COMe	9.0	9.6	16	3.0
23	F	OMe	CH	N	COMe	COMe	8.6	9.4	9	2.8
24	F	OMe	N	COMe	COMe	CH	*nd*	9.7	8	2.8
25	F	OMe	CH	N	COMe	CNHMe	8.9	9.2	7	0.3
26	F	F	N	COMe	COMe	CH	7.6	8.8	16	1.4
27	F	F	CH	N	COMe	COMe	7.7	8.6	23	1.4
28	-	-	-	-	-	-	< 5.2	< 5.0	*nd*	4.0

Table 3. RLM and PK parameters of **18-20**, **26** and **27** in rat and beagle. [a] Dosed at 1 & 2 mg/kg iv / po respectively in rat (2 & 2 mg/kg in beagle), using 10% DMA, 10% Solutol HS15, 80% Saline as vehicle. [b] Dosed at 1 & 2 mg/kg iv / po respectively in the rat PK studies (1 & 1 mg/kg in beagle), using 10% DMA, 10% Solutol HS15, 80% (10% aqueous (2-hydroxypropyl)-β-cyclodextrin) as vehicle. [c] *BQL* = Below quantifiable limit of 1.00 ng/mL.

			iv				po			
	RLM $t_{1/2}$ (min)	Species	Cl (mL/min/kg)	V_{ss} (L/kg)	Brain:Plasma (0.5 h)	CSF:Brain (0.5 h)	$t_{1/2}$ (po) (h)	AUC_{inf} (ng/h/mL)	T_{max} (h)	F_{po} (%)

18 [a]	28	Rat Beagle	18 5	2.2 3.6	0.77 -	0.01 -	1.6 10.6	558 6957	1.5 0.4	29 100
19 [a]	15	Rat	17	3.9	1.51	*BQL* [c]	3.3	705	0.4	36
20 [a]	23	Rat	34	3.5	0.79	0.02	1.8	300	0.8	29
26 [a]	16	Rat	29	2.3	0.84	0.01	1.3	401	0.5	34
27 [b]	23	Rat Beagle	18 13	2.1 3.0	0.49 -	0.01 -	1.8 7.1	1217 2442	0.5 0.4	66 70

Table 4. Profile of **27**. [a] See ESI† for assay details. [b] 1A2, 2C8, 2C9, 2C19, 2D6 and 3A4 isoforms. [c] Caco-2 monolayer, P_{app} A-B. [d] Binding to human, canine and murine plasma proteins respectively. [e] 5 strains, with and without S9 fractions.

OX_1 pK_i 7.7 [a] OX_2 pK_i 8.6 [a]	Permeability [c] $52x10^{-6}$ cm s^{-1} (efflux ratio 0.7)
OX_1 pK_b 6.6 [a] OX_2 pK_b 7.3 [a]	PPB% [d] 99.3, 98.1, 99.2
OX_1 kinetics: $t_{1/2}$ 0.8 min (SPR) OX_2 kinetics: $t_{1/2}$ 4.2 min (SPR), 7.6 min (biochemical)	Hepatocyte $t_{1/2}$: > 110 min (rat, dog), > 250 min (cyno, human)
P450 inhibition $pIC_{50} < 5$ [b]	No reactive metabolites
hERG $pIC_{50} < 5$	Ames Negative [e]